

Interplay of Conformational States and Nonbonded Interactions in Substituted Bithiophenes

Guido Raos,* Antonino Famulari, Stefano V. Meille, Maria C. Gallazzi, and Giuseppe Allegra

Dipartimento di Chimica, Materiali e Ingegneria Chimica "G. Natta", Politecnico di Milano, Via L. Mancinelli 7, 20131 Milano, Italy

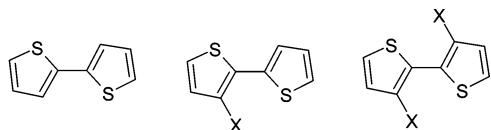
Received: September 2, 2003; In Final Form: November 18, 2003

We present ab initio calculations of the conformational effects produced by substitution of α,α' -bithiophene with fluorine, methoxy, methyl, or chlorine groups in one or both β positions (T_2X and T_2X_2). We find that the fluorine and methoxy substituents enhance the coplanarity of the rings in the trans conformation, while methyl and chlorine depress it by causing greater distortion. We also present the results of an atoms-in-molecules analysis of the molecular electron densities (bond and ring critical points). The $C_\alpha-C_\alpha'$ bond lengths and bond orders do not support the hypothesis that these conformational effects may be due to a π conjugation effect involving the substituents. On the other hand, we show that the planarization effects of the fluorine and methoxy substituents are mainly due to favorable intramolecular $S\cdots O$ and $S\cdots F$ nonbonded interactions. We also identify weak $CH\cdots O$ and $CH\cdots F$ interactions, stabilizing the planar cis states of the monosubstituted dimers. The changes in the $X-C_\beta-C_\alpha$ and $X-C_\beta-C_{\beta'}$ bond angles, indicating whether the X substituent distorts toward or away from the other ring in the planar conformations, are also in agreement with our interpretation.

Introduction

After a quarter of a century of research into organic conductors and semiconductors,^{1,2} oligo- and polythiophenes have established themselves as one of the most interesting classes of materials for organic electronics and optoelectronics.^{3–5} The introduction of substituents on the thiophene rings represents a simple and effective way to modulate their chemical and physical properties. The tuning of some important single-chain properties (ionization potential, electron affinity, electronic excitation spectrum, etc.) through the introduction of electron-donating or electron-withdrawing substituents follows a long-established tradition in physical organic chemistry and is apparently well understood³ (see ref 6 for a modern quantum chemical study along this line of thought). Other factors, particularly having to do with many-chain interactions (molecular packing in crystals and solid-state morphology, for example), are less under control. The main reason is that our knowledge of intermolecular forces as well as crystal nucleation and growth is still far from complete, despite the emergence of some important guiding principles from supramolecular chemistry and crystal engineering.⁷ It is apparent that the introduction of side groups also plays a role in processability and interaction with substrates.

The present work deals with the conformational states of bithiophene derivatives, as a function of the type and degree of substitution. In particular, we describe ab initio calculations of the torsion energy profiles of 2,2'-bithiophenes with a range of substituents in one or both 3 positions ($X = CH_3, Cl, F, OCH_3$):



* To whom correspondence should be addressed. Phone: +39-02-2399-3051. Fax: +39-02-2399-3080. E-mail: guido.raos@polimi.it.

Henceforth, we use T_2 , T_2X , and T_2X_2 to denote the unsubstituted, monosubstituted, and disubstituted bithiophenes, respectively. The alkyl side chains have been extensively studied before because of their ability to improve the solubility and self-assembly properties of the polymer and oligomers. However, they also increase the conformational disorder of the main chain, with a detrimental effect on the intramolecular π conjugation and charge transport properties. Alkoxy and fluorine substituents are instead expected to produce greater ring coplanarity in the minimum-energy transoid conformation.^{4,8} Interest in fluoro-substituted oligothiophenes has culminated in the recent synthesis and characterization of perfluorohexathiophene.⁹ The main motivation for the study of the chlorine derivatives is that this element has steric properties comparable to those of the CH_3 moiety, but at the same time, the two substituents clearly differ electrochemically.

Some of our calculations reproduce previous results on unsubstituted,^{10–14} alkyl-substituted,^{15,16} and alkoxy-substituted¹⁷ bithiophenes, while to our knowledge the conformational energies of fluorine- and chlorine-substituted bithiophenes have not been computed before. Even in the former cases, we provide some new numerical results, applying, for example, the MP2 method with a high-quality basis set. Apart from these numerical results, the main focus and novelty of the present study is the search for a quantum-chemical interpretation of the energetic and geometric effects produced by substitution. *Steric conflict* between adjacent rings is an obvious first candidate as driving force for conformational effects. Conjugation between the substituents and the rings affects the π electron distribution of the latter and may in principle lead to an increase of the *inter-ring C–C bond order*, and hence to a greater coplanarity. Finally, *attractive intramolecular nonbonded interactions* between the divalent sulfur and an electron-rich atom have been claimed to be important for the stabilization of the trans-planar conformation of alkoxy-substituted⁸ and carbonyl-substituted¹⁸ thiophenes. To clarify this issue, we rely mainly on Bader's "atoms in molecules" (AIM) analysis¹⁹ of the electron density

to highlight and characterize all the important bonded and nonbonded interactions between the rings.

The plan of the paper is as follows. In the next section we give details of the computational methods. Afterward we introduce those features of the AIM theory which are relevant in the present context. We then present our numerical results and their interpretation. In the conclusions we summarize our findings and briefly discuss them in a broader context.

Calculations

Previous *ab initio* calculations^{10–14} of the conformational states of T₂ have demonstrated the existence of two stable conformational minima around $\phi \cong \pm 150^\circ$ (“trans distorted”, TD, the absolute minimum) and $\phi \cong \pm 40^\circ$ (“cis distorted”, CD, at higher energy), where ϕ denotes the inter-ring S–C–C’∠S’ torsion angle. The structures at $\phi = 180^\circ$ (“trans planar”, TP) and at $\phi = 0^\circ$ (“cis planar”, CP) are actually transition states for the internal rotations, respectively bridging two symmetry-related TD or CD minima. Finally, there is an additional transition state (TS) at $\phi \cong \pm 90^\circ$, connecting a TD and a CD minimum. Reference 10 contains a review of the gas- and condensed-phase measurements which, despite some differences (between theory and experiment, but also among different experimental techniques) as to the height of the TS barrier or the TD–CD energy difference, confirm this qualitative picture. See in particular refs 20 and 21 for important gas-phase electron diffraction and spectroscopic data, respectively.

We searched for all the stationary points on the potential energy profile associated with torsion about the inter-ring C–C bond. Thus, we typically performed five geometry optimizations on each molecule: (i) unconstrained search (*C*₁ or *C*₂ symmetry, depending on the number of substituents) for the TD and CD conformational minima, (ii) constrained search (*C*_s, *C*_{2v}, or *C*_{2h} symmetry) of the TP and CP “minima”, (iii) transition-state search at $\phi \cong 90^\circ$, again with *C*₁ or *C*₂ symmetry. Some variations to this general scheme were imposed by qualitative changes in the potential produced by the introduction of the substituents.

In all cases, we carried out Hartree–Fock²² geometry optimizations with a standard 6-31G* basis set.²³ We shall refer to these as “RHF” results. The same geometries were also reoptimized at the MP2/6-31G** level²⁴ (henceforth “MP2”) and at the B3LYP/6-31G** level²⁵ (henceforth “B3LYP”). For the latter we adopted atom-based spherical grids for the integration of the exchange–correlation functional, with $96 \times 18 \times 36$ points distributed along the (*R*, θ , ϕ) polar coordinates. Calculations on T₂ by us¹⁴ and others^{12,13} show that the MP2 method is much more sensitive than RHF and B3LYP to the size and quality of the basis. Therefore, we performed a further set of single-point MP2 calculations with a spherical harmonic aug-cc-pVDZ basis,²⁶ at the MP2/6-31G** geometries (henceforth “large-MP2”). As will be seen, we do find substantial variations in the MP2 profiles on going from the 6-31G** to the aug-cc-pVDZ basis. Our calculation of T₂¹⁴ shows relatively minor changes in the MP2 torsion potential on further increasing the basis set to aug-cc-pVTZ. We suspect that this sensitivity of the MP2 method to the basis set is not due to some peculiar “correlation effect”, but more probably to an unbalanced treatment of intramolecular nonbonded interactions (the basis set superposition error^{27,28}).

The GAMESS-US program was used for all the calculations.²⁹

Synopsis of the AIM Theory

We briefly summarize those features of the AIM theory which are directly relevant for the present study.¹⁹ No attempt is made toward rigor and generality. In particular, the terms within quotes below have a special technical meaning, but here we prefer to bypass their definition and rely on their analogy with intuitive chemical concepts (indeed, the very existence of this analogy is one of the main reasons for the popularity of the method). See also refs 30 and 31 for representative applications of the AIM theory to hydrogen-bonded complexes, ref 32 for van der Waals complexes, ref 33 for sterically crowded molecules (ortho-substituted biphenyls), ref 34 for intramolecular chalcogen–chalcogen interactions, and ref 35 for CH⋯HC interactions in aromatic hydrocarbons.

The AIM theory focuses on the topological properties of the electron density function $\rho(\mathbf{r})$. This may be obtained either theoretically from a quantum-chemical calculation or experimentally from high-quality X-ray diffraction data.³⁶ The gradient vector field $\nabla\rho(\mathbf{r})$ is inspected, to track all the possible “bond paths” or “interaction lines” connecting all the “atom” pairs. This is a mathematically well-defined process, which does not involve any preconceived ideas about the existence of a bond between two atoms. It is reassuring that the “molecular graph” (the set of all bond paths) thus obtained is often isomorphous to the familiar Lewis-type representation of the molecular structure. However, bond paths may also be associated with nonbonded interactions, as will be seen shortly.

A “bond critical point” (BCP) is a stationary point of the electron density function (i.e., $\nabla\rho(\mathbf{r}) = 0$ at a BCP) located along a bond path. The value of the electron density at a BCP (ρ_B) may be taken as an indicator of the strength of the bond. In particular, for covalent C–C bonds it is possible to define a bond order n_{CC} on the basis of the following expression:¹⁹

$$n_{CC} = \exp[A(\rho_B - B)]$$

where *A* and *B* are positive constants, whose value is determined by requiring $n_{CC} = 1$ in ethane, 1.6 in benzene, and 2 in ethene.³⁷ At a more qualitative level, a rough correspondence between the BCP density and interaction strength can be established also for intermolecular interactions. In hydrogen-bonded complexes, the value of ρ_B on the donor–acceptor bond path is typically 100 times lower than in a covalent bond, being comprised between 2×10^{-3} au (weak H-bond) and 3.5×10^{-2} au (strong H-bond).³⁰ In a prototypical van der Waals complex such as Ar₂, $\rho_B = 2.9 \times 10^{-3}$ au at the equilibrium geometry.³² Another example is the global minimum of the (SO₂)₂ complex, which displays an S⋯O interaction with $\rho_B = 7.7 \times 10^{-3}$ au (this is the largest value, among all the heavy-atom “van der Waals bonds” examined in ref 32).

At a BCP, the electron density is minimum along the direction defined by the bond path, and maximum in the plane orthogonal to it. A BCP is thus a saddle point of the density, characterized by two negative eigenvalues and one positive eigenvalue of the Hessian matrix $\mathbf{H}_B = \nabla^T \nabla \rho(\mathbf{r})|_B$ (we take them such that $\lambda_1 \leq \lambda_2 < 0 < \lambda_3$). The Laplacian of the density is $\nabla^2 \rho_B = \text{Tr}(\mathbf{H}_B) = \lambda_1 + \lambda_2 + \lambda_3$. A negative Laplacian is the signature of a shared-electron covalent bond, whereas a positive Laplacian is typical of an interaction between closed-shell atoms.^{19,32} The values of $\nabla^2 \rho_B$ for a hydrogen bond are comprised between 2.4×10^{-2} and 14×10^{-2} au.³⁰ Those for a van der Waals bond are generally smaller and fall within a narrower range, between 1.2×10^{-2} au (for Ar₂) and 3.1×10^{-2} au (for the S⋯O interaction in (SO₂)₂).³² Finally, the ellipticity $\epsilon = \lambda_1/\lambda_2 - 1$

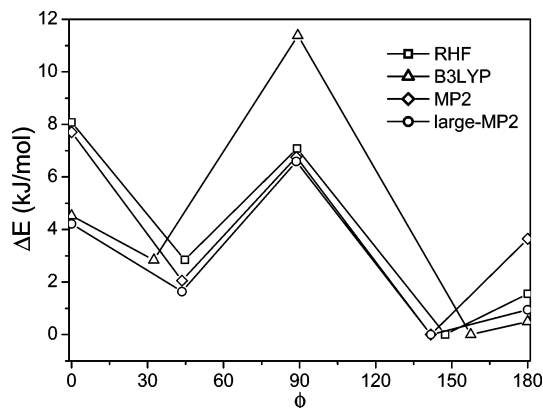


Figure 1. Conformational stationary points of T_2 .

characterizes the anisotropy of the charge distribution, in the directions orthogonal to the bond. It is zero in ethane and ethine (cylindrical symmetry of the bond), whereas it is about 0.40 in ethene and 0.22 in benzene.

A mathematical theorem (the Poincaré–Hopf relationship^{19,38}) ensures that the formation of a closed loop in the molecular graph (following, for example, a change in conformation, bringing two nonbonded atoms “in contact”) is accompanied by the simultaneous appearance of a “ring critical point” (RCP). This is again a stationary point of the electron density, with one negative eigenvalue and two positive eigenvalues of the Hessian (i.e., $\lambda_1 < 0 < \lambda_2 \leq \lambda_3$). The values of the electron density and its Laplacian at an RCP and the distance from a BCP to an RCP have also been used to characterize inter- and intramolecular nonbonded interactions.^{30,32–34}

The AIM analyses to be presented below were performed on both the MP2/6-31G** and the B3LYP/6-31G** electron densities, using Bader’s AIMPAC program.³⁹

Results and Discussion

Figure 1 contains a graphical summary of our results on the torsional energy of T_2 . The previously described qualitative picture of the conformational states is confirmed by all the calculations. We duly find the TD and CD minima, the TS connecting them at about 90° , and the planar TP and CP stationary points. Here and in the following figures, relative energies (ΔE) have been computed with respect to the lowest energy state, which in this case corresponds to TD. The quantitative differences among the computational methods have been extensively discussed before.^{12–14} We briefly summarize them, mainly to obtain a general feeling for their relative strengths and weaknesses. Overall, RHF is rather close to MP2, except for the relative energies of the TP and TD states. As a matter of fact, concerning this particular point, it is MP2 and not RHF which disagrees with large-MP2 and B3LYP. The gas-phase spectroscopic data²¹ actually support the latter, with a reported TP–TD energy difference of only 0.30 kJ/mol (our B3LYP value is 0.50 kJ/mol). B3LYP and large-MP2 also agree in predicting a small CP–CD energy difference. There is thus a larger degree of ring coplanarity than previously suspected, on the basis of early MP2 calculations with a moderately sized basis set.^{10,11} B3LYP departs from the other methods (and experimental evidence) by predicting a much higher torsional barrier at 90° . Note that full geometry optimizations at the MP2/aug-cc-pVDZ level¹⁴ have a minor effect on the relative energies of the TP, TS, and CP states, but may change somewhat the TD and CD energies by locating these minima at different values of the torsion angle (closer to the B3LYP/6-31G** values). All

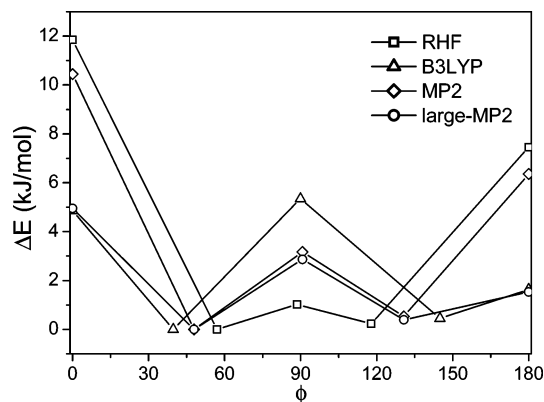


Figure 2. Conformational stationary points of T_2CH_3 .

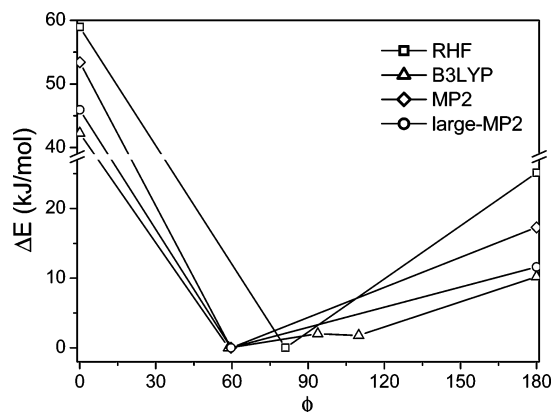


Figure 3. Conformational stationary points of $T_2(CH_3)_2$.

these *computational* trends are confirmed by the results on the substituted bithiophenes, to be discussed below. Taken together, without overemphasizing the results from a particular method but looking at the overall trends, these calculations can then be used to shed light on the qualitative changes produced by substitution.

Figures 2 and 3 illustrate the effect of substitution by methyl (or, more generally, alkyl) groups.^{15,16} With one methyl (T_2CH_3), the TD and CD states become very close in energy (< 1 kJ/mol) and the height of the barrier separating them is halved with respect to T_2 (from 7 to 3 kJ/mol for MP2 and from 11 to 5.5 kJ/mol for B3LYP). As in T_2 , B3LYP and large-MP2 agree in predicting planar states at relatively low energies, in contrast to RHF and MP2. The two distorted minima merge and the intermediate TS disappears on going to $T_2(CH_3)_2$. They survive as separate minima only at the B3LYP level, presumably because of the general tendency of this method to overestimate the height of the “intrinsic” barrier at 90° . The two methyls are only 4.03 (RHF), 3.46 (B3LYP), and 3.38 (MP2) Å apart, in the minimum-energy CD conformation. Comparing these figures with the van der Waals radius of methyl (2.00 Å, as given by Pauling⁴⁰), we see that this geometry results from the balance of inter-ring π conjugation and optimization of the $CH_3 \cdots CH_3$ interaction. The very high energy of the CP state of $T_2(CH_3)_2$ is obviously a consequence of the steric conflict between the methyls. The $CH_3 \cdots S$ interactions in the TP state are also repulsive, but to a lesser degree (consistently with the low-energy TP state observed in T_2CH_3).

The chlorine substituent behaves similarly to the methyl. In T_2Cl (see Figure 4), we find two distorted CD and TD minima with similar energies, separated by a low-energy TS. Again, high-energy CP and TP states are predicted by RHF and MP2, but their ΔE values are considerably reduced on going to large-

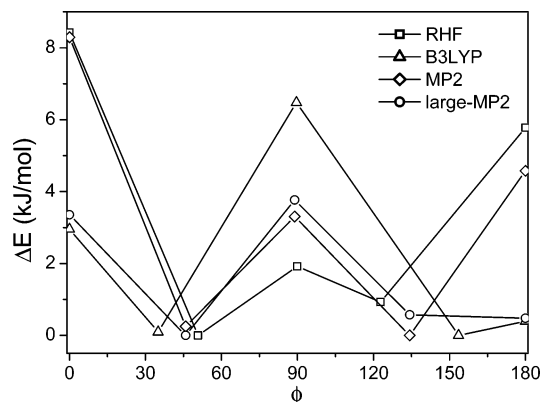


Figure 4. Conformational stationary points of T_2Cl .

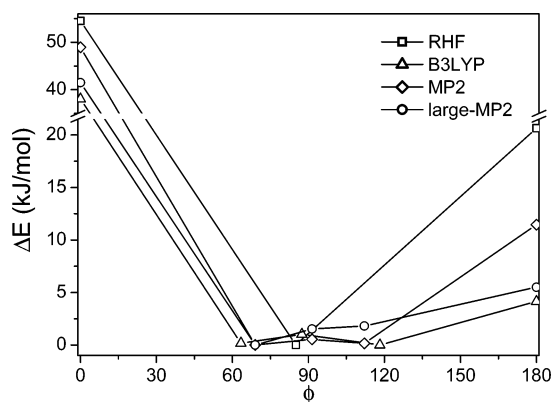


Figure 5. Conformational stationary points of T_2Cl_2 .

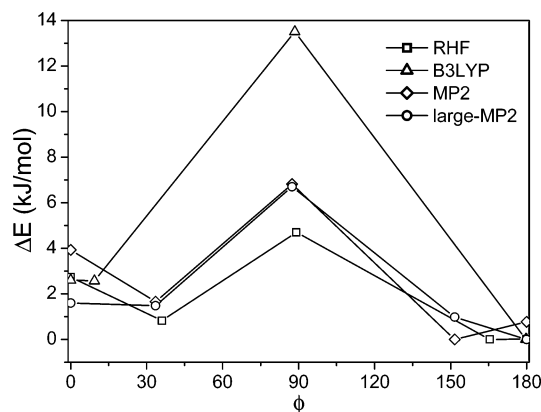


Figure 6. Conformational stationary points of T_2F .

MP2 and B3LYP. Indeed, the TD–TP energy difference and the ϕ_{TD} angle are almost identical to those of T_2 , at the B3LYP level. Of course, this similarity between T_2 and T_2Cl can only result from the balance of several contrasting effects. With two chlorines (T_2Cl_2 ; see Figure 5), the 90° barrier disappears (completely or almost completely, depending on the level of calculation) and the two distorted minima tend to merge, presumably giving a very flat profile of the potential around 90° . We see once more substantial agreement between B3LYP and large-MP2, in the prediction of TD states at relatively low energies (unlike RHF and MP2).

Substitution with one fluorine atom (T_2F ; see Figure 6) appears to flatten the energy profile about the TD and CD states. At the RHF and MP2 levels, they are distinct but very close in energy to the planar TP and CP states. They actually merge with them at the B3LYP level, and very likely also at the large-MP2 one (the uncertainty follows from the fact that these

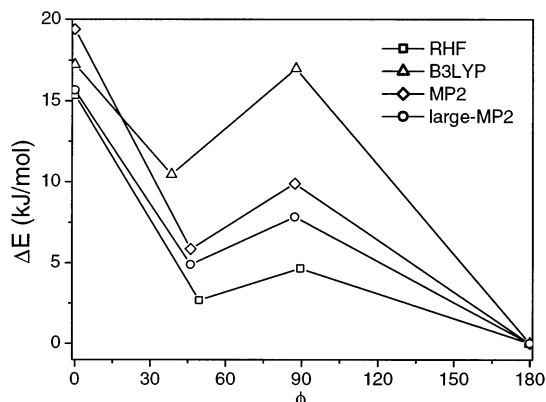


Figure 7. Conformational stationary points of T_2F_2 .

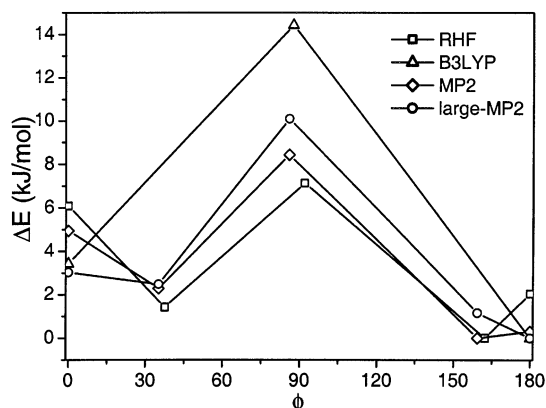


Figure 8. Conformational stationary points of T_2OCH_3 .

calculations did not involve any optimization, but were carried out at the geometries from the smaller basis set). Below we shall argue that this flattening is mainly due to favorable intramolecular $S\cdots F$ (for TP) and $CH\cdots F$ (for CP) interactions. The fact that the cis–trans relative energies are rather similar to those of T_2 (2–3 kJ/mol) suggests that these interactions are roughly comparable in strength. The TP and TD states actually merge in the difluorinated dimer, at all levels of theory (Figure 7). On the other hand, the CP and CD states are destabilized on going from T_2F to T_2F_2 , due to a combination of steric and electrostatic repulsion between the fluorines.

Overall, the methoxy substituent is fairly similar to fluorine, promoting ring coplanarity in the trans-like conformations. The flexibility of the side chains brings some additional complications. Thus, the OMe groups tend to lie out of the thiophene plane at the RHF level, whereas they stay in the plane at the B3LYP and MP2 levels. Clearly, these methods give different weights to the energy gain by conjugation of the oxygen lone pair with the π system of thiophene. The RHF global minimum is found at $\phi = 162^\circ$ in the monosubstituted dimer (T_2OCH_3 ; see Figure 8). The TP state is only 2 kJ/mol higher in energy, to be compared with 4 kJ/mol in T_2 (RHF level; see again Figure 1). The enhancement of coplanarity by the OMe group is confirmed by the B3LYP calculations, which predict fully planar TP and CP minima, with a relatively high barrier separating them. The MP2 calculations agree with RHF as to the TS barrier height, but confirm the B3LYP picture of coplanar cis and trans states (especially with the large basis set). Similarly, the disubstituted dimer ($T_2(OCH_3)_2$, Figure 9) has a global RHF minimum at $\phi = 168^\circ$, with a TP state only 0.15 kJ/mol higher in energy (C_i symmetry, with out-of-plane methoxys on opposite sides of the molecular plane; note that Figure 9 does not contain an RHF curve, due to difficulties encountered in the location

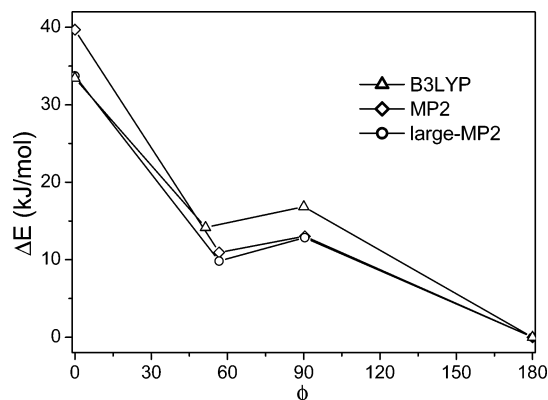


Figure 9. Conformational stationary points of $T_2(\text{OCH}_3)_2$.

TABLE 1: AIM Analysis on MP2/6-31G** Electron Densities: Local Properties at the Inter-ring C–C BCPs for Selected Geometries of the Systems under Investigation^a

system	D_{CC}	$10^2\rho_B$	n_{CC}	$10^2\nabla^2\rho_B$	$10^2\lambda_1$	$10^2\lambda_2$	$10^2\lambda_3$	ϵ	
T_2	TP	1.449	27.7	1.26	-70.2	-54.9	-48.6	33.3	0.131
	TD	1.450	27.7	1.26	-70.3	-54.3	-49.2	33.2	0.104
	TS	1.460	27.2	1.21	-68.0	-50.7	-50.5	33.2	0.003
	CD	1.451	27.6	1.25	-69.8	-53.9	-49.2	33.2	0.095
	CP	1.452	27.7	1.25	-68.4	-54.5	-48.2	33.3	0.130
T_2F	TP	1.446	27.7	1.26	-69.8	-54.7	-48.1	33.1	0.137
	TS	1.456	27.1	1.20	-67.8	-50.6	-50.3	33.0	0.006
T_2F_2	TP	1.442	27.7	1.26	-69.4	-54.6	-47.7	33.0	0.143
	TS	1.451	27.3	1.22	-67.7	-50.4	-50.1	32.9	0.006
$T_2\text{OCH}_3$	TP	1.445	27.8	1.27	-69.8	-55.0	-48.0	33.1	0.146
	TS	1.455	27.2	1.21	-67.9	-50.7	-50.2	33.0	0.011
$T_2(\text{OCH}_3)_2$	TP	1.441	27.8	1.27	-69.2	-54.9	-47.3	32.9	0.161
	TS	1.450	27.3	1.22	-67.8	-50.4	-50.3	32.9	0.001
$T_2\text{CH}_3$	TP	1.450	27.6	1.25	-69.2	-54.5	-47.9	33.3	0.139
	TS	1.460	27.1	1.20	-67.8	-50.6	-50.4	33.2	0.003
$T_2(\text{CH}_3)_2$	TP	1.453	27.4	1.23	-67.8	-54.0	-47.0	33.2	0.148
	CD	1.454	27.4	1.23	-68.6	-52.6	-49.1	33.2	0.007
$T_2\text{Cl}$	TP	1.449	27.6	1.25	-69.0	-54.4	-47.8	33.2	0.140
	TS	1.456	27.3	1.22	-68.2	-50.7	-50.6	33.0	0.003
$T_2\text{Cl}_2$	TP	1.452	27.3	1.22	-67.4	-53.8	-46.7	33.1	0.152
	TS	1.452	27.4	1.23	-68.5	-50.8	-50.7	33.0	0.003

^a C–C inter-ring distance (D_{CC} , Å), electron density at the BCP (ρ_B , au), C–C bond order (n_{CC}), Laplacian ($\nabla^2\rho_B$, au), eigenvalues λ_1 , λ_2 , and λ_3 , and ellipticity ϵ .

of the TS state). Bringing the OMe into the molecular plane (C_{2h} symmetry) costs an additional 4 kJ/mol. The TP state with in-plane OMe groups is instead the global minimum at the B3LYP and MP2 levels. Repulsive O···O interactions heavily destabilize the CP state, but a local CD minimum is nonetheless found by the RHF, MP2, and B3LYP methods.

According to the results presented so far, the substituents can be roughly divided into two groups, with fluorine and methoxy favoring ring coplanarity (unless there are two of them, interacting repulsively in the CP state of T_2X_2), while methyl and chlorine produce the opposite effect. It is natural to ask whether this can be related to their π -withdrawing/donating ability, their bulkiness, their electrostatic interactions, or whatever else. As anticipated in the Introduction, we have used Bader's AIM analysis of the electron density to address this question.

Tables 1 and 2 contain the geometrical and BCP data for the inter-ring C–C bonds, calculated from the MP2 and B3LYP densities. While the precise numerical values may change on going from one to the other method, the main trends are identical, and therefore, we do not distinguish between them in the following discussion. Let us first look in some detail at unsubstituted T_2 . The BCP electron density is large and the

TABLE 2: AIM Analysis on B3LYP/6-31G** Electron Densities: Local Properties at the Inter-ring C–C BCPs for Selected Geometries of the Systems under Investigation^a

system	D_{CC}	$10^2\rho_B$	n_{CC}	$10^2\nabla^2\rho_B$	$10^2\lambda_1$	$10^2\lambda_2$	$10^2\lambda_3$	ϵ	
T_2	TP	1.453	27.8	1.27	-70.0	-55.6	-49.1	34.9	0.132
	TD	1.452	27.8	1.27	-69.8	-55.3	-49.3	34.9	0.123
	TS	1.467	27.0	1.20	-66.4	-50.7	-50.6	34.8	0.001
	CD	1.454	27.7	1.26	-69.3	-54.9	-49.3	35.0	0.114
	CP	1.451	27.7	1.26	-69.1	-55.2	-48.8	34.9	0.132
T_2F	TP	1.447	27.8	1.27	-69.5	-55.5	-48.7	34.7	0.139
	TS	1.462	27.0	1.20	-77.8	-50.5	-50.3	34.7	0.003
T_2F_2	TP	1.444	27.8	1.27	-69.1	-55.4	-48.3	34.6	0.147
	TS	1.457	27.1	1.21	-66.1	-50.5	-50.2	34.5	0.006
$T_2\text{OCH}_3$	TP	1.447	27.9	1.28	-69.4	-55.7	-48.4	34.7	0.149
	TS	1.462	27.1	1.21	-66.0	-50.7	-50.0	34.7	0.013
$T_2(\text{OCH}_3)_2$	TP	1.444	27.9	1.28	-68.6	-55.5	-47.6	34.6	0.164
	TS	1.457	27.1	1.21	-65.8	-50.2	-50.2	34.5	0.000
$T_2\text{CH}_3$	TP	1.453	27.7	1.26	-68.8	-55.2	-48.4	34.8	0.141
	TS	1.467	27.0	1.20	-66.0	-50.5	-50.3	34.8	0.005
$T_2(\text{CH}_3)_2$	TP	1.457	27.4	1.24	-67.1	-54.5	-47.4	34.8	0.149
	TS	1.468	26.9	1.19	-65.6	-50.4	-50.0	34.7	0.010
$T_2\text{Cl}$	TP	1.452	27.6	1.25	-68.4	-55.0	-48.1	34.7	0.142
	TS	1.464	27.1	1.21	-66.6	-50.7	-50.5	34.7	0.003
$T_2\text{Cl}_2$	TP	1.455	27.3	1.22	-67.3	-53.8	-46.7	33.1	0.151
	TS	1.461	27.1	1.21	-66.7	-50.8	-50.5	34.6	0.006

^a See footnote a of Table 1.

Laplacian is negative, as expected for a covalent bond. Rotation from TP to TS is accompanied by a lengthening of the C–C bond and a reduction of the critical density and bond order. The bond length decreases and the bond order increases again on going further, from TS to CP. All this is quite reasonable, although these effects are smaller than what one might have naively expected. In particular, the bond order in the TS state is still relatively large (≈ 1.20) and close to the TP and CP values (≈ 1.26). On the other hand, there is little doubt that the C–C bond has lost all its π character in the TS state, as demonstrated by the (near) vanishing of the bond ellipticity ϵ (to be compared with 0.13 for the two planar states). All this can be rationalized by recognizing that even a $C(\text{sp}^2)\text{--}C(\text{sp}^2)$ "single" bond can be significantly stronger than the $C(\text{sp}^3)\text{--}C(\text{sp}^3)$ bond of ethane used as a reference.

Similar variations of the C–C bond lengths and orders are observed in the substituted bithiophenes, as a function of inter-ring twisting (only the TP and TS values are given for conciseness). The heavily crowded molecules, namely, $T_2(\text{CH}_3)_2$ and $T_2\text{Cl}_2$, represent two interesting exceptions. Especially at the MP2 level (but also, to a lesser degree, for B3LYP), these quantities are almost unchanged on going from TP to TS. A plausible explanation is that rotation about the C–C bond disrupts the π conjugation but, at the same time, alleviates the steric conflict which "stretches" the bond in the planar state.

While the above observations agree with our qualitative views about inter-ring π conjugation and its effect on the torsional barrier (relative energies of the TS and planar states), they do not answer our original question about the nature of the substituents and their stabilizing/destabilizing effect in the neighborhood of the planar conformations. Let us thus look again at Tables 1 and 2, keeping the conformational state fixed (we use TP for definiteness) and comparing the properties of the different molecules. On one hand, the C–C bond lengths seem to correlate nicely with the observed conformational effects. There is a shortening of D_{CC} for the "planarizing" substituents (i.e., $T_2 > T_2F > T_2F_2$, and similarly for $-\text{OCH}_3$) and a lengthening for the "distorting" ones (i.e., $T_2 < T_2\text{Cl} < T_2\text{Cl}_2$, and similarly for $-\text{CH}_3$). On the other hand, things get more complicated when we consider the BCP descriptors. The ρ_B and n_{CC} values are virtually unchanged by the $-\text{F}$ and

TABLE 3: AIM Analysis on MP2/6-31G Electron Densities: Selected Properties at the BCPs and RCPs for the X...Y Interactions^a**

system		X...Y	D_{XY}	C_{XY}	$10^2\rho_B$	$10^2\nabla^2\rho_B$	$10^2\rho_R$	$10^2\nabla^2\rho_R$	D_{BR}
T ₂ F	TP	F...S	2.934	0.92	1.16	4.97	1.00	5.52	0.504
	CP	F...H	2.342	0.92	1.18	5.21	0.87	5.05	0.641
T ₂ F ₂	TP	F...S	2.922	0.91	1.18	5.07	1.02	5.62	0.505
	CP	F...F	2.561	0.95	1.56	7.01	0.69	4.44	0.820
T ₂ OCH ₃	TP	O...S	2.870	0.88	1.49	5.19	1.13	5.88	0.632
	CP	O...H	2.301	0.88	1.48	5.34	0.96	5.16	0.738
T ₂ (OCH ₃) ₂	TP	O...S	2.830	0.87	1.62	5.59	1.19	6.26	0.656
	CP	O...O	2.625	0.94	1.73	6.00	0.71	3.77	0.905
T ₂ Cl	TP	Cl...S	3.211	0.88	1.22	4.47	0.92	4.39	0.684
	CP	Cl...H	2.587	0.86	1.28	4.79	0.81	3.95	0.804
T ₂ Cl ₂	TP	Cl...S	3.109	0.85	1.49	5.43	1.02	5.00	0.754
	CP	Cl...Cl	3.170	0.88	1.44	5.55	0.55	2.33	1.090

^a D_{XY} = X...Y distance (Å); $C_{XY} = D_{XY}/(R_X + R_Y)$ = contraction ratio with respect to the sum of the van der Waals radii of X and Y (Pauling values⁴⁰); ρ_B = electron density at the BCP (au); $\nabla^2\rho_B$ = Laplacian at the BCP (au); ρ_R = electron density at the RCP (au); $\nabla^2\rho_R$ = Laplacian at the RCP (au); D_{BR} = distance of the RCP from the BCP (Å).

TABLE 4: AIM Analysis on B3LYP/6-31G Electron Densities: Selected Properties at the BCPs and RCPs for the X...Y Interactions^a**

system		X...Y	D_{XY}	C_{XY}	$10^2\rho_B$	$10^2\nabla^2\rho_B$	$10^2\rho_R$	$10^2\nabla^2\rho_R$	D_{BR}
T ₂ F	TP	F...S	2.950	0.92	1.10	4.62	0.94	5.24	0.506
	CP	F...H	2.361	0.93	1.11	4.84	0.83	4.81	0.633
T ₂ F ₂	TP	F...S	2.942	0.92	1.12	4.69	0.96	5.30	0.503
	CP	F...F	2.576	0.95	1.44	6.39	0.67	4.24	0.807
T ₂ OCH ₃	TP	O...S	2.906	0.89	1.36	4.72	1.04	5.47	0.625
	CP	O...H	2.345	0.90	1.33	4.79	0.88	4.78	0.722
T ₂ (OCH ₃) ₂	TP	O...S	2.864	0.88	1.49	5.09	1.09	5.82	0.651
	CP	O...O	2.678	0.96	1.52	5.10	0.65	3.48	0.882
T ₂ Cl	TP	Cl...S	3.233	0.89	1.16	4.24	0.86	4.19	0.701
	CP	Cl...H	2.618	0.87	1.20	4.46	0.75	3.73	0.809
T ₂ Cl ₂	CP	Cl...S	3.129	0.86	1.43	5.17	0.95	4.79	0.769
	CP	Cl...Cl	3.203	0.89	1.34	5.19	0.50	2.17	1.094

^a See footnote a of Table 3.

–OCH₃ substituents, *despite* the shortening of the C–C bond length. These quantities decrease very slightly for –Cl and –CH₃, possibly *as a consequence* of the lengthening of the C–C bond. The bond ellipticities ϵ (index of the π character) always increase, independently of the nature of the substituent (i.e., T₂ < T₂X < T₂X₂ for any X). Thus, there is no clear signature in the electronic structure at the C–C BCPs that inter-ring conjugation represents the *driving force* for planarization of the fluorine- and methoxy-substituted bithiophenes.

Tables 3 and 4 summarize our AIM results on the intramolecular nonbonded interactions in the CP and TP states (for MP2 and B3LYP densities, respectively). With the exception of unsubstituted T₂, all the molecules are “sterically crowded”³³ in their TP and CP conformations (we do not present the data on T₂CH₃ and T₂(CH₃)₂, because of the complications introduced by the internal structure of the methyl group). The presence of a BCP for a given nonbonded interaction is associated with an RCP and a contact distance below the sum of the van der Waals radii⁴⁰ (see the C_{XY} ratios in Tables 3 and 4), and vice versa. It is significant that the C_{SH} ratio takes the value of 1.03 in the TP conformation of T₂, and in agreement with this observation we do not find any S...H interaction line. Similarly, we never find a H...H interaction line (unlike planar biphenyl^{33,35}). Again, there is overall consistency between the properties (densities and Laplacians) from the MP2 and B3LYP methods, with the former yielding slightly larger values than the latter (for a given system and geometry). Thus, the main trends may be equally inferred from one or the other set of calculations.

The densities at the S...F and S...O BCPs fall between 1.1×10^{-2} and 1.6×10^{-2} au. These values are 50–100% larger than those calculated by Bone and Bader for weak van der Waals

complexes,³² and they are actually in the typical range of moderately strong hydrogen bonds. The Laplacian values are narrowly distributed about 5×10^{-2} au, above those quoted by Bone and Bader³² and within the range of hydrogen bonds.³⁰ The positive sign of the Laplacian indicates a contraction of the electron density toward the interacting nuclei and away from the BCPs, and the locally dominant role of the kinetic over the potential energy.^{19,32} These properties are consistent with van der Waals or closed-shell S...F and S...O interactions. It is also interesting to consider their relative strengths. The contact distance contractions are approximately 12% and 8%, respectively, for –OCH₃ and –F (incidentally, optimization of these interactions seems to be the likely source of the C–C bond shortening discussed above). Also, ρ_B values for the S...O interactions are $\cong 20\%$ higher than the S...F ones. The energy difference between the TP states (maximum S...X interaction) and the TS states (minimum S...X interaction) provides one final piece of evidence: this is about 10 kJ/mol in T₂F, to be compared with 12 kJ/mol in T₂OCH₃ (averages of large-MP2 and B3LYP values). Taken together, these observations indicate that the S...O interaction is stronger than the S...F one. Going back to Tables 1 and 2, we also observe that the ρ_B values and equilibrium S...F distances of T₂F₂ are rather similar to those of T₂F. On the other hand, we see a 10–15% increase of ρ_B and a significant shortening (–0.04 Å) of the S...O distance, on going from T₂OCH₃ to T₂(OCH₃)₂. These suggest a cooperative mutual strengthening of the S...O interactions in the disubstituted dimer, which does not occur with the fluorines.

Further intramolecular O...HC and F...HC interactions are detected in the CP states of T₂OCH₃ and T₂F. The BCP properties for the former fall within the previously discussed range.³⁰ The F...HC critical point has a smaller density and

TABLE 5: Values of the Bond Angles α and β and of the Distortion Parameter Δ^a in the Symmetrically Substituted Bithiophenes^b

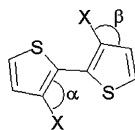
system		α (deg)	β (deg)	Δ (deg)
T ₂	TP	122.77; 122.85	124.01; 123.47	-1.52; -1.12
	TS	122.10; 122.24	124.85; 124.16	
T ₂ (CH ₃) ₂	CP	122.76; 122.92	124.04; 123.44	-1.48; -1.23
	TS ^c	124.08; 124.52	124.17; 123.24	
T ₂ Cl ₂	CP	129.55; 129.56	118.32; 117.97	-11.32; -10.32
	TP	125.66; 125.68	119.52; 118.86	-6.28; -5.37
T ₂ F ₂	TS	122.93; 123.36	123.06; 121.91	
	CP	128.62; 128.56	117.00; 116.44	-11.75; -10.67
T ₂ (OCH ₃) ₂	TP	121.82; 121.99	122.46; 121.94	0.36; 0.94
	TS	122.27; 122.63	122.55; 121.68	
T ₂ (OCH ₃) ₂	CP	124.07; 124.11	120.69; 120.23	-3.67; -2.89
	TP	118.79; 119.38	127.15; 126.32	0.11; 0.60
T ₂ (OCH ₃) ₂	TS	119.22; 119.96	127.47; 126.30	
	CP	121.73; 122.09	124.84; 124.23	-5.13; -4.30

^a See the text for their definition. ^b For each table entry, the first number corresponds to MP2/6-31G**, the second one to B3LYP/6-31G**. ^c There is no TS state for T₂(CH₃)₂, at the MP2/6-31G** level (see again Figure 3). We have obtained the α and β values from the CD geometry, in this case.

Laplacian, consistently with the fact that organic fluorine is known to be a very weak acceptor of hydrogen bonds.⁴¹ These interactions justify the lowering and flattening of torsion potential in the neighborhood of the CD-CP states.

As mentioned above, BCPs are detected also in the cases which had been previously classified as “repulsive”, such as the CP conformations of T₂F₂ (F···F interaction), of T₂(OCH₃)₂ (O···O interaction), and of T₂Cl₂ (Cl···Cl interaction). The electron density and Laplacian at these BCPs are comparable (or even higher) to those for the “attractive” interactions. However, the properties at the ring critical points discriminate very clearly between the two situations. The repulsive cases are characterized by lower values of ρ_R ((0.5–0.7) × 10⁻² au, compared to (0.9–1.2) × 10⁻² au for the attractive ones) and larger BCP-RCP distances (D_{BR} in Tables 3 and 4). Similar conclusions were reached in a comparative study of chalcogen–chalcogen and hydrogen-bonding interactions,³⁴ where a linear relationship was established between ρ_R and other measures of the interaction strength (enthalpy of isodesmic reactions and contraction of intramolecular contact distances).

To sum up, the AIM analysis supports the conclusion that the inter-ring conjugation cannot be considered the main driving force for planarization, although it is certainly important as far as the TS barrier height is concerned. Instead, specific inter-ring intramolecular interactions seem to be the most important factor. As an additional check of this conclusion, we have monitored the distortion of the $\alpha = X-C_\beta-C_\alpha$ and $\beta = X-C_\beta-C_{\beta'}$ bond angles in the symmetrically substituted bithiophenes (see Table 5):



A value of $\alpha < \beta$ corresponds to a distortion of the X substituent toward the opposite ring. Two of us⁸ took this structural feature as an indicator of an attractive S···O interaction in alkoxythiophenes (at the experimental TP geometry, in the solid state). An even more convincing proof comes from the *variation* of $\alpha - \beta$ as a function of conformation (there may be several possible reasons for $\alpha \neq \beta$: the two angles can be significantly different

even in the substituted thiophene *monomer*). Thus, the last column of Table 5 contains the following quantities:

$$\Delta = (\beta - \alpha)_{TP/CP} - (\beta - \alpha)_{TS}$$

A value of $\Delta > 0$ means that the X substituent bends toward the opposite ring, on going from the orthogonal to a planar conformation (i.e., attractive interactions). Indeed, we observe positive Δ values in the TP states of T₂F₂ and T₂(OCH₃)₂ and negative Δ values in all the other cases, which had been classified as repulsive. The fact that the negative Δ values are, in absolute value, much larger than the positive ones is quite understandable, considering the generic shape of a nonbonded potential energy curve (i.e., comparable displacements from the equilibrium distance produce strong repulsive forces and relatively weak attractive ones). Finally, note the slightly negative Δ values in the TP and CP states of unsubstituted T₂, which according to the present criterion may be associated with mildly repulsive S···HC and CH···HC interactions (for which, however, there is no BCP).

Before closing this section, we briefly recall some previous studies, pointing to the directional character of nonbonded interactions involving divalent sulfur. Statistical surveys of crystallographic data⁴² have highlighted a preferential mode of interaction with electron-rich groups, which tend to approach the sulfur *in the molecular plane*, 30–60° off the C_{2v} axis (of a ring). This pattern closely resembles the S···X arrangement in the TP states of fluorine- and alkoxy-substituted bithiophenes. On the other hand, electrophilic centers⁴² tend to bind to the sulfur *out of the molecular plane*, 50–60° from thiophene's C_{2v} axis. This effect was rationalized in terms of lone-pair angular correlations by a spin-coupled study of furan and thiophene,⁴³ which was mainly concerned with the unusual “bent” S-coordination of the latter to transition-metal cations.⁴⁴ Relatively simple electrostatic models, accounting for directionality and anisotropy through distributed multipoles,²⁷ also proved useful in explaining the markedly different mode of interaction of furan and thiophene with HF and HCl,⁴⁵ as well as the geometry of thiophene–thiophene gas-phase complexes.⁴⁶ Work is currently under way in our laboratory to include these effects in empirical force fields for oligo- and polythiophenes.

Summary and Conclusions

We have presented ab initio calculations of the conformational effects produced by substitution of 2,2'-bithiophene (T₂) with one or two fluorine, methoxy, methyl, or chlorine groups, in one or both 3 positions. Compared to unsubstituted T₂, which adopts a minimum-energy trans-distorted conformation in the gas phase, we have found that the fluorine and methoxy substituents enhance the coplanarity of the rings, whereas methyl and chlorine behave similarly by producing greater distortion. Thus, our calculations indicate that the introduction of alkoxy or fluorine groups onto the backbone of poly- and oligothiophenes has a potentially beneficial effect on the inter-ring π conjugation and related properties, such as intramolecular charge transport.⁴⁷

We have also investigated the origin of the conformational effects produced by the substituents. As a note of caution, we point out that the rigorous quantum-chemical interpretation of the origin of torsional barriers is a controversial subject⁴⁸ which is still being actively pursued on systems as simple as ethane, sometimes with results which challenge our understanding of “steric interactions”.^{35,49} Instead of attempting a decomposition of the total energy into a force-field-like sum of

stretching, bending, torsion, electrostatic, and van der Waals contributions, we have used Bader's atoms-in-molecules analysis of the electron density¹⁹ to characterize the most important bonded and nonbonded interactions within these molecules. We find that stabilization of the planar conformations by the fluorine and alkoxy groups is *not due* (or mainly due) to a conjugation effect (i.e., an increase of the π bond order between the rings). Rather, we detect inter-ring S \cdots O and S \cdots F (in the trans-planar states) or CH \cdots O and CH \cdots F (in the cis-planar states of the monosubstituted dimers) bond critical points, showing that the main driving force toward coplanarity is represented by *specific nonbonded interactions* between an electron-rich substituent and the sulfur or hydrogen atoms on the other ring. The changes in the X-C $_{\beta}$ -C $_{\alpha}$ and X-C $_{\beta}$ -C $_{\beta'}$ bond angles, indicating whether the X substituents distort toward or away from the other ring in the planar conformations, confirm our interpretation. This is also in agreement with previous discussions of alkoxythiophenes and 1,2-difluoro-1,2-bis(2-thienyl)ethenes by two of us, which were mainly based on solid-state structural evidence.^{8,50} We suggest that the same interactions may be exploited to gain greater control not only over the conformational state of individual molecules, but also over intermolecular interactions and packing in crystals.⁷

Acknowledgment. We thank Chiara Castiglioni for her interest and encouragement, one reviewer for useful suggestions, and our former student Giulia Moschieri for some preliminary AIM results. This work was financially supported by MIUR-COFIN2002. Part of the calculations were carried out thanks to a grant of computer time by Cilea and Politecnico di Milano.

References and Notes

- (1) Shirakawa, H.; Louis, E. J.; MacDiarmid, A. G.; Chiang, C. K.; Heeger, A. J. *J. Chem. Soc., Chem. Commun.* **1977**, 578. Chiang, C. K.; Park, Y. W.; Heeger, A. J.; Shirakawa, H.; Louis, E. J.; MacDiarmid, A. G. *Phys. Rev. Lett.* **1977**, 39, 1098.
- (2) Shirakawa, H. *Angew. Chem., Int. Ed.* **2001**, 40, 2574. MacDiarmid, A. G. *Angew. Chem., Int. Ed.* **2001**, 40, 2581. Heeger, A. J. *Angew. Chem., Int. Ed.* **2001**, 40, 2591.
- (3) Roncali, J. *Chem. Rev.* **1992**, 92, 711.
- (4) *Handbook of Oligo- and Polythiophenes*; Fichou, D., Ed.; Wiley-VCH: Weinheim, Germany, 1999.
- (5) Fichou, D. *J. Mater. Chem.* **2000**, 10, 571.
- (6) Salzner, U.; Kızıltepe, T. *J. Org. Chem.* **1999**, 64, 764.
- (7) Lehn, J. M. *Supramolecular Chemistry: Concepts and Perspectives*; Wiley-VCH: Weinheim, Germany, 1995. Desiraju, G. R. *Angew. Chem., Int. Ed. Engl.* **1995**, 34, 2311. Gavezzotti, A. *Modell. Simul. Mater. Sci. Eng.* **2002**, 10, R1.
- (8) Meille, S. V.; Farina, A.; Bezziccheri, F.; Gallazzi, M. C. *Adv. Mater.* **1994**, 6, 848.
- (9) Sakamoto, Y.; Komatsu, S.; Suzuki, T. *J. Am. Chem. Soc.* **2001**, 123, 4643.
- (10) Ortí, E.; Viruela, P.; Sánchez-Marín, J.; Tomás, F. *J. Phys. Chem.* **1995**, 99, 4955.
- (11) Viruela, P. M.; Viruela, R.; Ortí, E.; Bredas, J. L. *J. Am. Chem. Soc.* **1997**, 119, 1360.
- (12) Karpfen, A.; Choi, C. H.; Kertesz, M. *J. Phys. Chem. A* **1997**, 101, 7426.
- (13) Duarte, H. A.; Dos Santos, H. F.; Rocha, W. R.; De Almeida, W. B. *J. Chem. Phys.* **2000**, 113, 4206.
- (14) Raos, G.; Famulari, A.; Marcon, V. *Chem. Phys. Lett.* **2003**, 379, 364.
- (15) Alemán, C.; Julia, L. *J. Phys. Chem.* **1996**, 100, 1524.
- (16) Bongini, A.; Bottoni, A. *J. Phys. Chem. A* **1999**, 101, 7426.
- (17) DiCésare, N.; Belletête, M.; Leclerc, M.; Durocher, G. *J. Mol. Struct.: THEOCHEM* **1999**, 467, 259.
- (18) Pomeranz, M. *Tetrahedron Lett.* **2003**, 44, 1563.
- (19) Bader, R. F. W. *Atoms in Molecules—A Quantum Theory*; Oxford University Press: Oxford, 1990. Bader, R. F. W. *Chem. Rev.* **1991**, 91, 893.
- (20) Samdal, S.; Samuelsen, E. J.; Volden, H. V. *Synth. Met.* **1993**, 59, 259.
- (21) Takayanagi, M.; Gejo, T.; Hanozaki, I. *J. Phys. Chem.* **1994**, 98, 12893.
- (22) Roothan, C. C. *J. Rev. Mod. Phys.* **1951**, 23, 69. Hall, G. G. *Proc. R. Soc. London* **1951**, A205, 541.
- (23) Hehre, W. J.; Ditchfield, R.; Pople, J. A. *J. Chem. Phys.* **1972**, 56, 2257. Hariharan, P. C.; Pople, J. A. *Chem. Phys. Lett.* **1972**, 66, 217. Franci, M. M.; Pietro, W. J.; Hehre, W. J.; Binkley, J. S.; Gordon, M. S.; DeFrees, D. J.; Pople, J. A. *J. Chem. Phys.* **1982**, 77, 3654.
- (24) Møller, C.; Plesset, M. S. *Phys. Rev.* **1934**, 46, 618. Pople, J. A.; Binkley, J. S.; Seeger, R. *Int. J. Quantum Chem. Symp.* **1976**, 10, 1. Dupuis, M.; Chin, S.; Marquez, A. In *Relativistic and Electron Correlation Effects in Molecules*; Malli, G., Ed.; Plenum Press: New York, 1994; p 315.
- (25) Becke, A. D. *J. Chem. Phys.* **1993**, 98, 5648. Stephens, P. J.; Devlin, F. J.; Chabrowski, C. F.; Frisch, M. J. *J. Phys. Chem.* **1994**, 98, 11623. Hertwig, R. H.; Koch, W. *Chem. Phys. Lett.* **1997**, 268, 345.
- (26) Dunning, T. H., Jr. *J. Chem. Phys.* **1989**, 90, 1007. Woon, D. E.; Dunning, T. H., Jr. *J. Chem. Phys.* **1993**, 98, 1358. Davidson, E. R. *Chem. Phys. Lett.* **1996**, 260, 514.
- (27) Stone, A. J. *The Theory of Intermolecular Forces*; Oxford University Press: Oxford, 2000.
- (28) Boys, S. F.; Bernardi, F. *Mol. Phys.* **1970**, 19, 553. van Duijneveldt, F. B.; van de Rijdt, J. G. C. M.; van Lenthe, J. H. *Chem. Rev.* **1994**, 94, 1873. Jeziorski, B.; Moszynski, P.; Szalewicz, K. *Chem. Rev.* **1994**, 94, 1887. Famulari, A.; Gianinetti, E.; Raimondi, M.; Sironi, M. *Int. J. Quantum Chem.* **1998**, 69, 151.
- (29) Schmidt, M. W.; Baldrige, K. K.; Boatz, J. A.; Elbert, S. T.; Gordon, M. S.; Jensen, J. H.; Koseki, S.; Matsunaga, N.; Nguyen, K. A.; Su, S. J.; Windus, T. L.; Dupuis, M.; Montgomery, J. A. *J. Comput. Chem.* **1993**, 14, 1347.
- (30) Koch, U.; Popelier, P. L. A. *J. Phys. Chem.* **1995**, 99, 9747. Popelier, P. L. A. *J. Phys. Chem. A* **1998**, 102, 1873. Hocquet, A. *Phys. Chem. Chem. Phys.* **2001**, 3, 3192.
- (31) Gatti, C.; Famulari, A. Interaction Energy and Density in the Water Dimer. A Quantum Theory of Atoms in Molecules Insight on the Effect of Basis Set Superposition Error Removal. In *Electron, Spin and Momentum Densities and Chemical Reactivity*; Mezey, P. G., Robertson, B. E., Eds.; Kluwer Book Series Understanding Chemical Reactivity, Vol. 21. Chapter 6; Kluwer: Dordrecht, The Netherlands, March 2000; hardbound, ISBN 0-7923-6085-0.
- (32) Bone, R. G. A.; Bader, R. F. W. *J. Phys. Chem.* **1996**, 100, 10892.
- (33) Cioslowski, J.; Mixon, S. T. *J. Am. Chem. Soc.* **1992**, 114, 4382.
- (34) Sanz, P.; Mó, O.; Yáñez, M. *Phys. Chem. Chem. Phys.* **2003**, 5, 2942.
- (35) Matta, C. F.; Hernández-Trujillo, J.; Tang, T.-H.; Bader, R. F. W. *Chem.—Eur. J.* **2003**, 9, 1940.
- (36) Koritsansky, T. S.; Coppens, P. *Chem. Rev.* **2001**, 101, 1583.
- (37) The precise numerical values of A and B depend on the method used to compute $\rho(\mathbf{r})$. For MP2/6-31G**, we have derived $A = 7.28$ au and $B = 0.246$ au. For B3LYP/6-31G**, we find $A = 6.68$ au and $B = 0.243$ au.
- (38) Collard, K.; Hall, G. G. *Int. J. Quantum Chem.* **1977**, 12, 623.
- (39) Available for download from <http://www.chemistry.mcmaster.ca/aimpac/>.
- (40) Pauling, L. *The Nature of the Chemical Bond*, 2nd ed.; Cornell University Press: Ithaca, NY, 1960.
- (41) Dunitz, J. D.; Taylor, J. D. *Chem.—Eur. J.* **1997**, 3, 89.
- (42) Rosenfield, R. E., Jr.; Parthasarathy, R.; Dunitz, J. D. *J. Am. Chem. Soc.* **1977**, 99, 4860. Guru Row, T. N.; Parthasarathy, R. *J. Am. Chem. Soc.* **1981**, 103, 477.
- (43) Mitchell, P. C. H.; Raos, G.; Karadakov, P. B.; Gerratt, J.; Cooper, D. L. *J. Chem. Soc., Faraday Trans.* **1995**, 91, 749.
- (44) Angelici, R. J. *Coord. Chem. Rev.* **1990**, 105, 61. Rauchfuss, T. B. *Prog. Inorg. Chem.* **1991**, 39, 259.
- (45) Cooke, S. A.; Corlett, G. K.; Lister, D. G.; Legon, A. C. *J. Chem. Soc., Faraday Trans.* **1998**, 94, 837. Cooke, S. A.; Corlett, G. K.; Legon, A. C. *Chem. Phys. Lett.* **1998**, 291, 269.
- (46) Tsuzuki, S.; Honda, K.; Azumi, R. *J. Am. Chem. Soc.* **2002**, 124, 12200.
- (47) Grozema, F. C.; van Dujinen, P. Th.; Berlin, Y. A.; Ratner, M. A.; Siebbeles, L. D. A. *J. Phys. Chem. B* **2002**, 106, 7791.
- (48) Goodman, L.; Pophristic, V.; Weinhold, F. *Acc. Chem. Res.* **1999**, 32, 983.
- (49) Pophristic, V.; Goodman, L. *Nature* **2001**, 411, 565.
- (50) Albertin, L.; Bertarelli, C.; Gallazzi, M. C.; Meille, S. V.; Capelli, S. C. *J. Chem. Soc., Perkin Trans. 2* **2002**, 1752.